Separated Trailing-Edge Flow at a Transonic Mach Number

P. R. Viswanath*
Stanford University, Stanford, California
and
J. L. Brown†
NASA Ames Research Center, Moffett Field, California

Results from an experimental investigation of a small-scale separated flow at a sharp trailing edge are presented. The separated flow was a result of sustained adverse pressure gradients. Experiments were carried out at a transonic Mach number, without any shock wave in the flow, and at a high Reynolds number. Measurements include surface pressure distributions, mean velocity, turbulent shear stress, turbulent kinetic energy, and some streamwise turbulence intensity profiles in the region from just upstream of separation to downstream into the near wake, following wake closure. The results show noticeable changes in the mean and turbulent quantities in the separated region although the wall adverse pressure gradients are relatively weak. Turbulent normal stress becomes important in the vicinity of separation and in the separated zone with regard to both mean flow development and turbulence energy production. The experimental data are used to assess the performance of simple algebraic turbulence models and two boundary-layer calculation methods.

Nomenclature

c_f = wall skin-friction coefficient, $2\tau_w/\rho_e U_e^2$
H = shape factor, δ^*/θ
ℓ_m = Prandtl mixing length
M = Mach number
P = static pressure
P_T = total pressure
Re = Reynolds number per meter
U = mean velocity in X direction
U_0 = sonic (reference) velocity
$\langle uv \rangle$ = mean velocity correlation
$\langle u^2 \rangle$ = mean square velocity fluctuation in X direction
$\langle v^2 \rangle$ = mean square velocity fluctuation in Y direction
X = streamwise coordinate parallel to model centerline measured from trailing edge of model
Y = vertical coordinate normal to model centerline measured from model surface and in the wake from the model trailing edge
γ_p = downstream intermittency
δ = boundary-layer thickness
δ_0 = reference boundary-layer thickness
δ^* = displacement thickness
ϵ = eddy viscosity
θ = momentum thickness
ρ = density
τ = shear stress

Subscripts

e = boundary-layer edge conditions
L = based on model length
n = nominal freestream conditions
w = wall

Introduction

TRAILING-edge boundary-layer separation, resulting from sustained adverse pressure gradients in the rear portions of airfoils and wings, occurs frequently.[1-3] Separation usually leads to an increase in drag and a reduction in lift. Viscous effects at transonic speeds are significant,[4,5] even under attached flow conditions, and proper treatment of the trailing-edge region, accounting for wake curvature, normal pressure gradients, and viscous-inviscid interactions is necessary to obtain satisfactory predictions[4] of lift and drag. Modern transonic airfoil shapes (e.g., rear-loaded supercritical airfoils) are such that the turbulent boundary layer grows rapidly toward the trailing edge, because of the large adverse pressure gradients, and the flow is often under nearly separating conditions. Small-scale trailing-edge separation is a common occurrence on these airfoils,[3,6] even under slight off-design conditions, and it can have appreciable effects on airfoil performance. At transonic Mach numbers, the problem may be more complex because of the presence of a shock wave on the upper surface, whose effects on the boundary layer generally promote trailing-edge separation.[5]

Successful predictions of the turbulent boundary-layer separation at high Reynolds number, and calculations of the separated flow, at least to engineering accuracy, depend greatly on satisfactory modeling of turbulence, as well as accounting for strong viscous-inviscid interactions. Currently, in most of the viscous-inviscid interactive calculation methods,[4,6,7] viscous effects are taken into account successfully through boundary-layer displacement thickness distributions on the airfoil and in the near wake. A similar treatment may be adequate, even with a small-scale separated flow at the trailing edge. However, our ability to calculate the mean turbulent flow, and consequently the displacement thickness, in strong adverse pressure gradients and in the separated region is not satisfactory,[6,8,9] a major deficiency being in the modeling of turbulent stresses in these complex flows. Navier-Stokes computations[10] also suffer from the inadequacy of turbulence modeling. Further progress relies very much on extracting information relevant to modeling from well-planned experiments involving turbulence measurements. A recent study[11] has provided some data on a supercritical airfoil with weakly separated trailing-edge flow, and has also revealed some of the complexities of the flow. It is the primary objective of the present work, to study in some detail, a small-scale trailing-edge separated flow on a relatively simple configuration with a view to understanding some of the basic features of the flow and to improve flow modeling.

Presented as Paper 82-0348 at the AIAA 20th Aerospace Sciences Meeting, Orlando, Fla., Jan. 11-14, 1982; submitted Jan. 22, 1982; revision received Aug. 9, 1982. This paper is declared a work of the U.S. Government and therefore is in the public domain.

*Research Associate, Department of Aeronautics and Astronautics, Joint Institute for Aeronautics and Acoustics. Member AIAA.
†Research Scientist. Member AIAA.

The experiment is conducted at a transonic Mach number and at a high Reynolds number of practical interest. The freestream conditions have been chosen so as to avoid the shock on the upper surface of the model, thus reducing the degree of complexity of the flow. Laser Doppler velocimetry is used for measuring mean and turbulence quantities throughout the flowfield, including the separated region. The experiment has also been designed, following some of the guidelines suggested in the recent Stanford Conference,[12] to be useful as a test case for evaluating turbulence models and prediction methods. This effort is a continuation of earlier studies[13,14] on unseparated trailing-edge flows.

The experimental results of mean and turbulence flowfield are presented. Observations of separated-flow characteristics, a discussion of mean-flow dynamics, and some data analysis related to turbulence modeling in the separated region are included. Results from boundary-layer computations are also presented.

Experiments

Experimental Setup and Test Conditions

The experiments were conducted in the 38.1×25.4-cm high Reynolds number channel blowdown facility at Ames Research Center (Fig. 1a). The model configuration, which spans the test section, is made up of two parts: 1) a forebody, which is a flat plate 56.75 cm long and 2.54 cm thick with a 24.51-cm-long tapered forward section having a rounded leading edge (Fig. 1b); and 2) an aft body sharp trailing-edge flap, which is 14.1-cm long. The cross section of the flap is the upper rear quadrant of an 18%-thick circular-arc airfoil; the arc has a radius of curvature of 40.4 cm and the trailing-edge included angle of the flap is 20.4 deg. The design of the flap was guided by our experience from earlier studies,[13,14] as well as by some of the criteria for turbulent boundary-layer separation suggested in the literature. The lower surface of the flap provides a zero pressure gradient boundary-layer flow thus minimizing the overall complexity of the flow. The model has these added advantages: 1) it provides a thick and fully developed turbulent boundary layer on the flat plate, which is desirable for modeling studies, and 2) the relatively long length of the model combined with the stagnation pressure available with the facility gives high Reynolds numbers, a unique feature of the present experiments.

Although the freestream Mach number was varied during the preliminary phase of the experiments, all detailed flowfield measurements were made at a nominal freestream Mach number M_n of 0.7 and at a Reynolds number (based on model length) Re_L of 40×10^6. This Reynolds number corresponds to a nominal total temperature of 470°R and a total pressure P_T of 275 kPa.

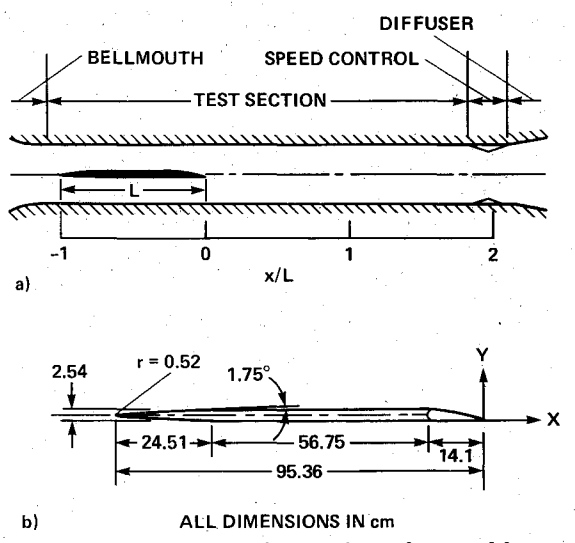

Fig. 1 Schematic of test section and test model.

Surface and Flowfield Measurements

The flat-plate flap model described has 75 static pressure orifices, most of which are located on the centerline of the model on both the upper and lower surfaces. Spanwise static pressure orifices were also provided to assess spanwise uniformity of surface pressures. Static pressure orifices were also provided on the top and bottom walls of the tunnel in the region of the model, as well as downstream to a distance of 45 cm. The pressures were measured with strain gage pressure transducers; each transducer was calibrated before each tunnel run.

Most flowfield measurements were made using a two-dimensional laser Doppler velocimeter (LDV) described previously.[13,14] The two channels of the LDV were operated independently in two beam orientations: 1) beams aligned at ±45 deg to the tunnel axis allowing measurements of U, V, $\langle uv \rangle$, and $\langle u^2 + v^2 \rangle$, and 2) beams aligned along and normal (0-90 deg) to the tunnel axis, thereby measuring U, V, $\langle u^2 \rangle$, and $\langle v^2 \rangle$. Most measurements, however, were carried out in the ±45 deg orientation; the 0-90 deg orientation was used only at selected stations where turbulence intensity measurements were desired. Some measurements using conventional pitot and static probes were also made. These probe pressures were measured by Statham pressure transducers.

The flow was visualized, using conventional Schlieren and shadowgraph methods, and the surface flow on the flap was examined, for example, for flow reversal and three-dimensional effects, using an oil-flow technique.

Accuracy of Measured Data

The various sources of error considered for the LDV measurements include optical, electronic, statistical, and positional. The accuracy assessment is based also on repetition of data points and comparison with velocity data derived from pitot-static measurements. The mean velocity is estimated to be accurate to ±4% or ±4 m/s, whichever is greater. Similarly, the turbulence quantities ($\langle uv \rangle$, etc.) are deemed accurate to ±8% or ±16 m^2/s^2, whichever is greater. Due to glare and low seed level, the greatest inaccuracies occur in the separation region close to the body surface. Positioning accuracy of the LDV system was found to be ±0.04 cm. More details on the accuracy assessment are described in Ref. 15.

Two Dimensionality of the Flowfield

Two dimensionality of the mean flow was validated, based on oil-flow patterns on the flap surface, observations of spanwise variations of certain flow quantities, and estimates of the two-dimensional boundary-layer momentum integral equation from the measured data.[16]

Results and Discussion

Mean Flowfield and Separation Characteristics

The initial phase of the experiments consisted of acquiring model static-pressure distributions to identify a suitable separated flow case for detailed flowfield measurements. This was achieved by varying the tunnel Mach number M_n in discrete steps, at constant total pressure P_T.

Figure 2 shows the static-pressure distributions, normalized by P_T, on the upper surface of the flap at three different Mach numbers. The static pressures on the lower (flat-plate) surface of the flap are also shown (dotted lines). At each M_n, a circulation develops around the model, and pressures on the upper and lower flat-plate portions (not shown) are nearly constant but at different levels. At all three values of M_n, the pressure on the upper surface first decreases (from the

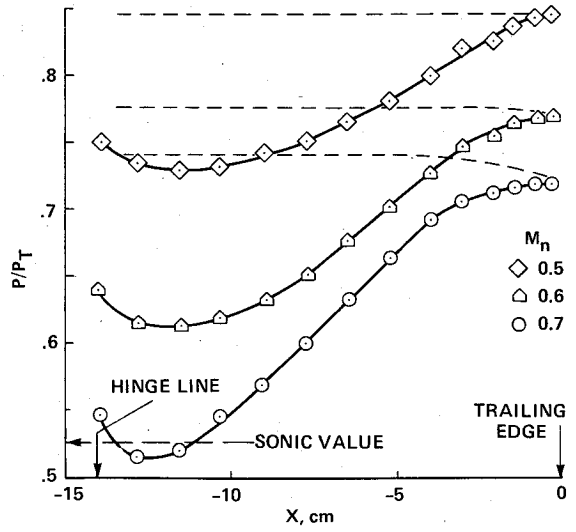

Fig. 2 Mach number effects on static pressure distributions: $P_T = 275$ kPa.

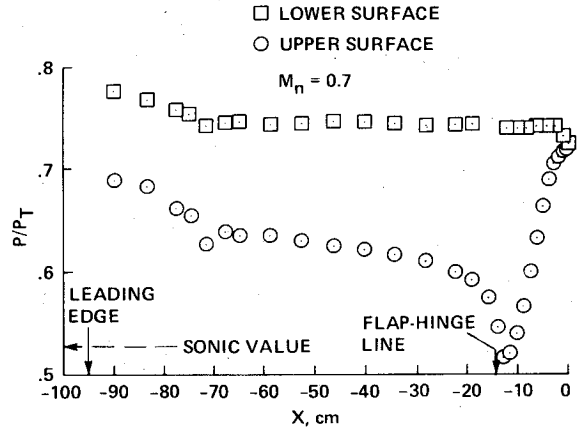

Fig. 3 Static pressure distributions on the model: $M_n = 0.7$, $Re_L = 40 \times 10^6$.

pressure level on the flat plate) toward the hinge line in response to the change in model curvature and then increases toward the trailing edge. The pressure gradient over the middle of the flap is nearly constant at each M_n, but this gradient does increase with M_n. The data also exhibit a relief in pressure gradients toward the trailing edge with increasing M_n, indicating separation of the boundary layer.[17] At $M_n = 0.5$, the boundary layer is probably attached; with increasing M_n, the separation forms at the trailing edge and moves upstream because of the increasing adverse pressure gradients. Surface oil-flow patterns on the flap confirmed these observations.[16] Further increases in M_n beyond 0.7, resulted in the formation of a shock downstream of the hinge line. On the lower surface, at $M_n = 0.6$ and 0.7, there is a weak acceleration of the flow over the flat plate toward the trailing edge in response to the reduced pressure recovery on the upper surface, resulting from the separated flow. The flow at $M_n = 0.7$ was selected for detailed flowfield measurements because it showed maximum length of separation and was shock free. The pressure distributions for the complete model at $M_n = 0.7$ are shown in Fig. 3.

A spark shadowgraph of the flowfield is shown in Fig. 4. The boundary layers and the wake can be distinguished from the background. Vortex-like structures, rotating counterclockwise, are being shed at the trailing edge on the lower surface; these result from the large velocity differences existing across the trailing edge. No such structures are seen on the upper surface, probably because of the reduced

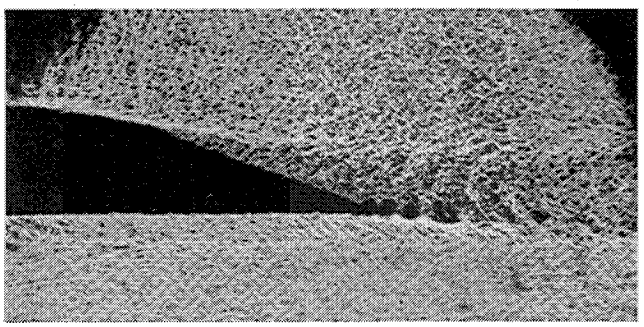

Fig. 4 Spark shadowgraph of the trailing-edge flowfield: $M_n = 0.7$, $Re_L = 40 \times 10^6$.

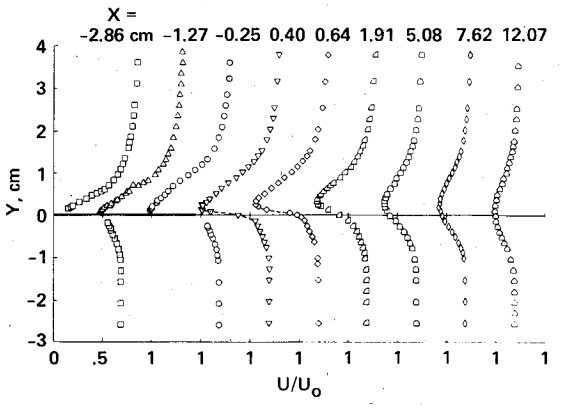

Fig. 5 Measured mean velocity profiles: $M_n = 0.7$, $Re_L = 40 \times 10^6$.

velocity gradients associated with the thicker separated boundary layer. Similar structures have been observed on unseparated asymmetric trailing-edge flows.[14] The existence of these structures could play an important role (e.g., new time and length scales) in the determination of the wake closure and in the development of the near wake.

The development of the turbulent boundary layers on the upper surface of the model and into the near wake is discussed next. Ahead of the flap, on the flat plate ($X = -27.3$ cm) the mean velocity profile measured showed good agreement with the law of the wall suggesting a fully developed turbulent boundary layer.[16] Over the initial part of the flap, the mean velocity development showed a continuous deceleration due to the adverse pressure gradients. All the mean and turbulent velocity profiles to follow are presented normalized by the sonic speed ($U_0 = 295.7$ m/s). The velocity profiles measured (with ± 45 deg LDV system) downstream through separation and in the near wake are shown in Fig. 5. Not all the measured profiles are shown for the sake of clarity. From all the measured velocity profiles, separation is inferred to have occurred in the range $-2.38 \le X \le -1.9$ cm. This location is consistent with the location at which flow reversal was inferred ($X_{fr} = -2.0 \pm 0.25$ cm) from surface oil-flow pattern.[16] The height of the reversed flow is small (≈ 0.20 cm) compared with the boundary-layer thickness. An interesting feature of the velocity field in the separated zone is that there are rapid changes (deceleration) all across the layer, although the wall adverse pressure gradient is very small.

Wake closure occurs downstream of the trailing edge at $X = 0.40$ cm. The quite rapid wake closure is a result of the interaction of the energetic lower side (flat-plate) flow with the separated shear layer on the upper surface. There is some evidence[3] that such rapid wake closure occurs downstream of the trailing edge even on supercritical airfoils. Downstream of wake closure, an asymmetric wake is formed. In the near wake only the velocities inner region (around minimum velocity) increases rapidly with distance while the outer regions of both the upper and lower sides show only small changes.

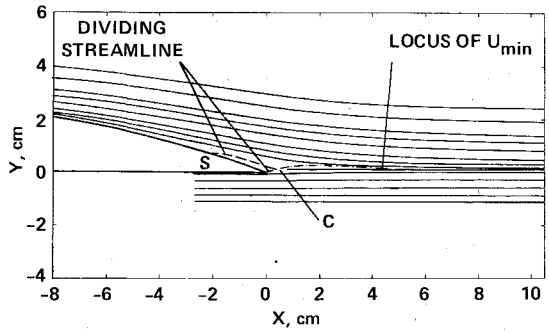

Fig. 6 Mean streamlines on the flap and in near wake: $M_n = 0.7$, $Re_L = 40 \times 10^6$.

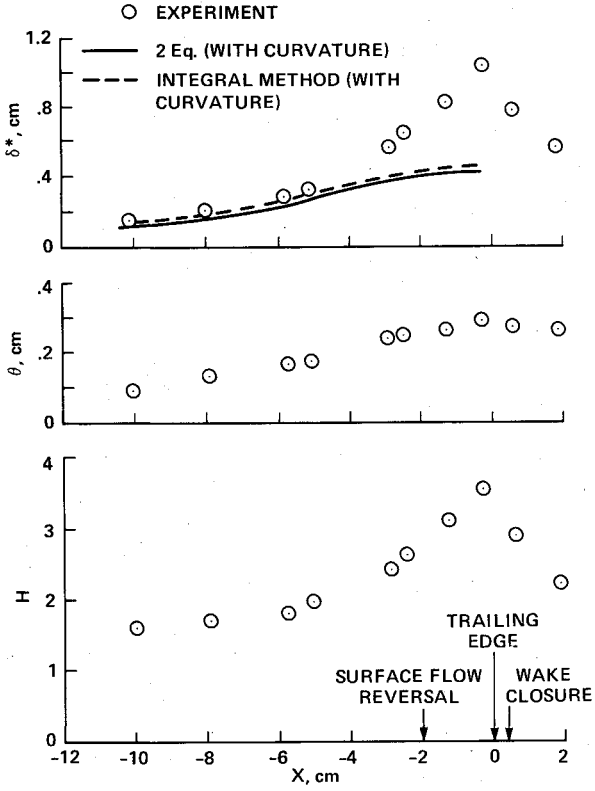

Fig. 7 Variation of boundary-layer integral thickness parameters: $M_n = 0.7$, $Re_L = 40 \times 10^6$.

Mean flow streamlines on the flap and in the near wake, calculated using the mass flow concept, are presented in Fig. 6. The separation point S, the wake closure C, and the dividing streamlines are also shown in the figure. Even though the height of the reversed flow is small, typically 4-5 data points could be obtained in the reversed flow at each X station, which were used to locate the dividing streamline on the upper surface.[16] The streamlines sketched downstream of the trailing edge are also only approximate.[16] A noticeable feature in the boundary layer on the flap upper surface is the significant reduction (compared to the surface) in the convexity of the mean streamlines, particularly close to the wall. This is a result of the continuously decelerating velocity field (giving diverging streamlines), which is a result of the adverse pressure gradient. Consequently, across the boundary layer, the static pressure changes in the region $-8 < X < 0$ cm are small; the estimated maximum pressure change was only about 5% of the wall pressure.

The variation in boundary-layer integral thickness parameters on the upper surface of the flap and in the upper part of the near wake is shown in Fig. 7. The integral thickness parameters are defined taking into account (in an approximate sense) the weak pressure variations across the boundary layer in a manner suggested in Ref. 18. The calculations shown in Fig. 7 will be discussed later. The rapid increase in δ^* and H toward the trailing edge and their rapid initial decay in the near wake may be clearly seen. These variations are typical of those found on airfoils at transonic speeds. The shape factor has a value of about 2.8 ± 0.1 at the surface-flow reversal location.

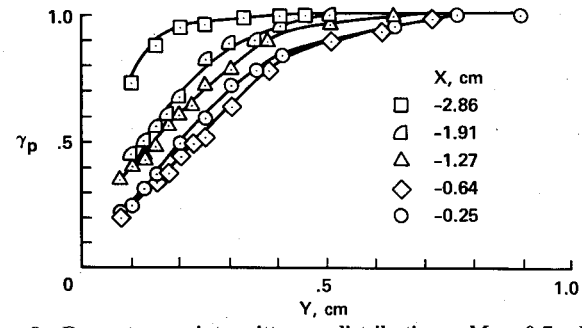

Fig. 8 Downstream intermittency distributions: $M_n = 0.7$, $Re_L = 40 \times 10^6$.

We next discuss a feature of the time-dependent nature of the flowfield in the vicinity of the separation point. One measure of the unsteady nature of separation is γ_p, defined as the fraction of the time the flow has a positive streamwise component. It was estimated from the measured data of streamwise velocity fluctuations in a manner similar to that of Simpson et al.[19] Measured U velocity distribution functions were used rather than an assumed Gaussian distribution. These results are presented in Fig. 8 for five different measurement stations. According to Refs. 19 and 20, intermittent separation point occurs for a value of γ_p near the wall of about 0.8, and fully developed separation point occurs at γ_p of about 0.5. Also, from Fig. 7 of Ref. 19, γ_p appears to be nearly constant in the inner 8-10% of the boundary-layer thickness. In the present experiments (Fig. 8) the first data point near the wall corresponds to about 0.05δ. If we assume the near constancy behavior of γ_p near the wall in the present flow, the preceding definitions imply intermittent separation at $X = -2.86$ cm and fully developed separation at $X = -1.91$ cm. This latter location ($X = -1.91$ cm) is consistent with the location at which surface-flow reversal was inferred ($X_{fr} = -2.0$ cm). The pressure-gradient relief, according to Fig. 2, has already begun slightly upstream of intermittent separation. There is broad agreement of these separation characteristics at this transonic condition with those observed at low speeds.

In this experiment, the turbulent boundary layer on the flap separates under the combined action of adverse pressure gradient and convex curvature, with the influence of the former the greater. The curvature of mean streamlines in the boundary layer is much smaller than at the surface. Since convex curvature of mean streamlines has the effect of reducing wall skin friction, even in a zero pressure-gradient flow,[21] boundary-layer separation in the present case may have resulted farther upstream compared with a curvature free flow with the same pressure gradient.

Turbulence Flowfield

As stated earlier, turbulent shear, kinetic energy and the two turbulent intensities were measured in the vicinity of separated region. Here we present only the shear stress and kinetic energy profiles.

Turbulent shear stress $-\langle uv \rangle$ profiles through separation and in the near wake are presented in Fig. 9. Since ρ variation across the boundary layer is only about 10%, ρ is neglected in the preceding definition of shear stress. The magnitude of shear stress increases, particularly in the outer part of the boundary layer, in the separation zone. The normal gradients

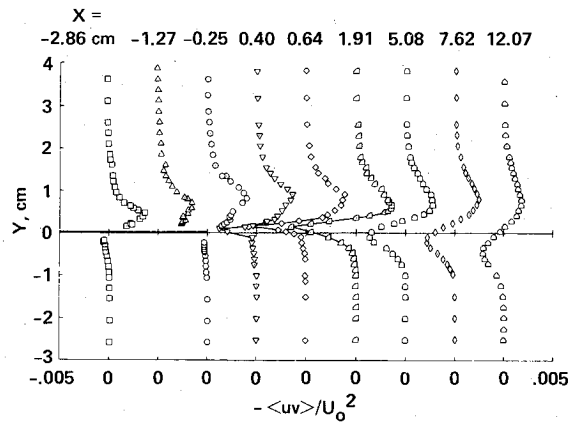

Fig. 9 Measured turbulent shear stress profiles: $M_n = 0.7$, $Re_L = 40 \times 10^6$.

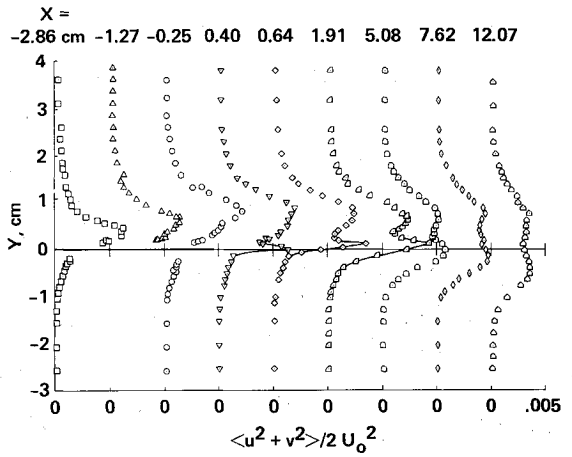

Fig. 10 Measured turbulent kinetic energy profiles: $M_n = 0.7$, $Re_L = 40 \times 10^6$.

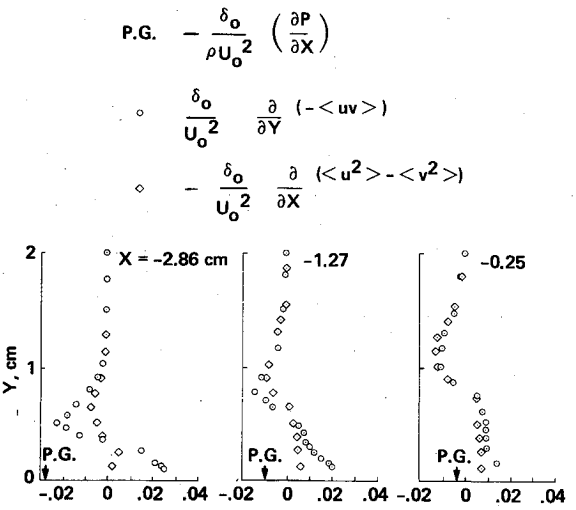

Fig. 11 Gradients of wall static pressure and Reynolds stresses: $M_n = 0.7$, $Re_L = 40 \times 10^6$.

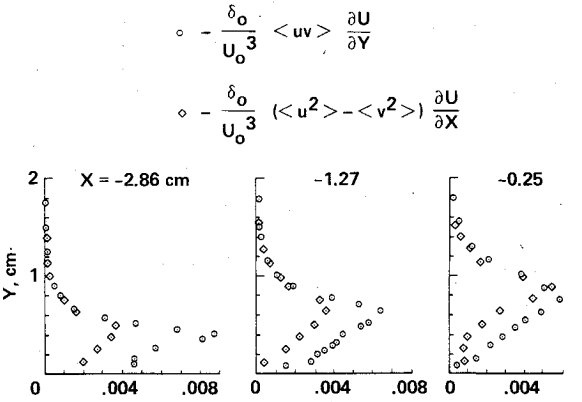

Fig. 12 Turbulence production owing to Reynolds stresses: $M_n = 0.7$, $Re_L = 40 \times 10^6$.

near the wall are decreasing progressively toward the trailing edge. This is a result of the continuous reduction in the wall pressure gradient. The Y location, say, Y_m, at which maximum shear stress occurs moves outward with increasing streamwise distance along the flap. Similar behavior is also seen with kinetic energy profiles, as we shall see later. This feature is often seen in adverse pressure-gradient boundary-layer flows.[22] In the separated region (for $-2 < X < 0$), this outward movement of Y_m could be attributed, at least partly, to the outward displacement of the mean streamlines because of the separated bubble.

In the near wake, following the wake closure, large normal gradients in shear stress develop, as a result of merging of shear layers. These gradients decrease farther downstream. In the narrow region, where the shear layers are merging, the shear stress varies nearly linearly with Y. The wake profiles show two peaks of differing sign, corresponding to the upper and lower sides of the wake. The magnitudes of these peaks decay as the flow moves downstream. The wake data also show that shear stress changes sign in the neighborhood of $\partial U/\partial Y = 0$. For this flow, the eddy viscosity concept to model Reynolds shear stress may be adequate. Many of these wake features are similar to those observed[13,14] in the unseparated asymmetric near wakes.

The two-component kinetic energy profiles are displayed in Fig. 10. The kinetic energy levels increase in the separated zone, particularly in the outer region. Similar behavior was also observed in the $\langle u^2 \rangle$ profiles.[16] In the near wake, large normal gradients develop like the shear stress profiles. Again, two peaks are seen in the near wake and they decay with distance downstream.

To obtain better insight into the dynamics of mean flow in the vicinity of the separated region, the different terms of the X momentum equation (including the turbulent normal stress but ignoring the small density variations) were estimated from the measured data after smoothing. Figure 11 shows these estimates of the nondimensional wall pressure gradient, Reynolds shear, and normal stress gradients at three streamwise locations. The first location ($X = -2.86$ cm) is just ahead of separation, and the other two stations are in the separated region.

The following observations can be made: 1) the streamwise wall pressure gradient decreases rapidly in the separated region; 2) in the wall region (say, $Y/\delta \leq 0.10$), transverse shear stress gradients are much larger than the streamwise normal stress gradients; and 3) in the outer region ($Y/\delta \geq 0.10$), the normal-stress gradients are comparable to the shear stress gradients, particularly in the separated region. These results show that away from the wall, the turbulent normal and shear stress gradients are significant to the mean flow development (deceleration) in the separated region. Further analysis (unpublished) shows that the normal stress is significant also in the region of wake closure.

The influence of turbulence normal stresses on turbulence production in the turbulence energy-transport equation is examined next. Nondimensional turbulent shear stress and normal stress production terms are estimated and presented in Fig. 12 at the same locations as Fig. 11. Production by normal stresses is significant at all three stations and is comparable in magnitude to the shear stress production. Maximum values of production at each streamwise location occur close to where

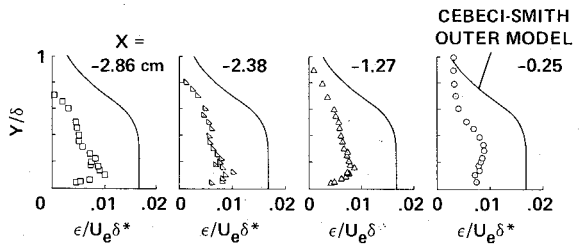

Fig. 13 Eddy-viscosity profiles: $M_n = 0.7, Re_L = 40 \times 10^6$.

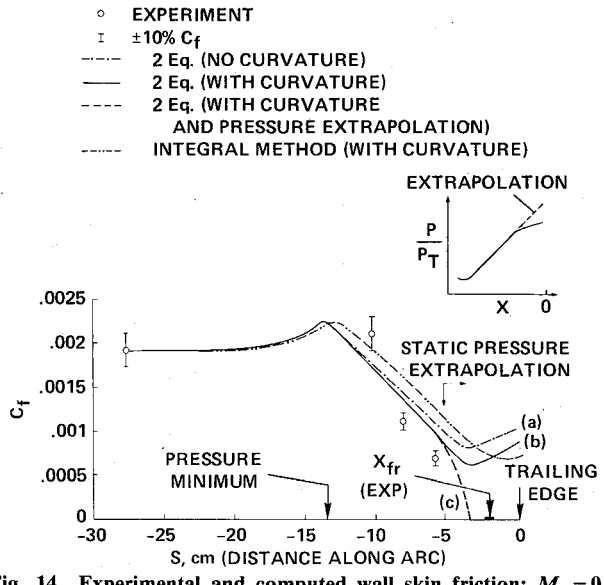

Fig. 14 Experimental and computed wall skin friction: $M_n = 0.7$, $Re_L = 40 \times 10^6$.

the shear stress and mean-velocity gradient ($\partial U/\partial Y$) reach maximum values. The turbulence production owing to normal stress probably accounts, in part, for the increased turbulent kinetic-energy levels (more in the width than peak value of the profiles) observed in the separated region. Simpson et al.[19] and Delery[23] have also emphasized recently the importance of turbulence normal stress in the streamwise momentum equation and in the production of turbulence in other separating flows.

To assess the utility of some of the algebraic eddy-viscosity models often used in engineering calculations, the eddy viscosity ϵ and Prandtl mixing length ℓ_m were calculated from the measured shear stress data and estimated mean velocity gradient. Here we show only the eddy viscosity distribution (Fig. 13) at four locations in the vicinity of the separated region. The value of U_e was determined from the measured surface pressure and isentropic flow relations. In the outer region, the nondimensional eddy viscosity ($\epsilon/U_e\delta^*$) distributions are reduced by nearly half from the Cebeci and Smith values[24] (with intermittency), which may be reasonably expected to be valid on the flat plate boundary layer ahead of the flap. Only small variations in these nondimensional eddy viscosity values are seen in the separated region. The smaller eddy viscosity levels may have resulted in part from the influence of convex curvature of mean streamlines on the flap boundary layer. Similar reduction in the nondimensional eddy viscosity levels have been observed[11] in progressing from about the midchord to the trailing edge on a supercritical airfoil with a weakly separated trailing-edge flow. However, their actual levels near the trailing edge are much higher (comparable to the Cebeci and Smith values) than those observed in the present study, possibly due to the significant differences in the upstream history of the boundary-layer flow (e.g., a shock wave on the airfoil), and in the flow Reynolds number between the two experiments. Similarly smaller nondimensional mixing lengths (ℓ_m/δ) compared to the flat plate boundary-layer values were seen in the outer region.[16]

Boundary-Layer Calculations

The performance of two boundary-layer calculation methods for the flow over the flap upper surface are assessed in the following. The first method uses a two equation eddy-viscosity model[25] and the second involves an integral method[26] widely used in transonic airfoil calculations. Both calculations are made using the measured surface pressure distributions after matching (within a few percent) the calculated δ^*, c_f with measured values at $X = -27.3$ cm on the flat plate.

Figure 14 shows comparisons of wall skin friction coefficient c_f on the upper surfaces of the flat plate and of the flap with boundary-layer computations. On the upper surface of the flap, the experimental wall shear stress was inferred by fitting the velocity data near the wall (obtained using a pitot probe) to the law of the wall.[16] The effect of curvature on c_f in the two-equation model calculations may be seen by comparing curves a and b. It is clear that separation is not predicted by the two-equation model calculations. Following Cebeci et al.,[17] the calculations were repeated with an extrapolated pressure distribution (extension of the linear portion, see Fig. 2, beyond $X = -4.0$ cm) and the results are also shown in Fig. 14 as curve c. As may be seen, c_f approaches zero at a location extremely close to the location at which minimum c_f occurred using the experimental pressure distribution. We infer calculated separation to be at $X = -3.2$ cm, which is about 0.5δ upstream of the experimental flow reversal point. The predictions of c_f from the integral method (Fig. 14) show variations qualitatively similar to that of the two-equation model results, and the separation point with the extrapolated pressure distribution was found to be close to measured X_{fr}. The results for separation location by either method, we believe, is at least as good as those obtained by Cebeci et al. at low speeds.

The displacement thickness predictions are included in Fig. 7. The calculations show good agreement up to $X = -5$ cm; however, because the calculations do not predict separation for the measured pressure distribution, the downstream predictions are appreciably lower than the data. The results from the integral method do not differ significantly from the boundary-layer calculations employing the two-equation model of turbulence. According to Ref. 26 the integral method is not expected to be accurate for $H \gtrsim 2.5$, which for present flow occurs around $X = -3$ cm. Similar underpredictions of δ^* near the trailing edge have been observed on supercritical airfoil studies (e.g., Ref. 27).

Concluding Remarks

To improve our understanding of some of the basic features of small-scale trailing-edge separated flows and to enable improved flow modeling of them, a detailed experimental study has been conducted. The experiments are conducted on an elongated airfoil-like model at a transonic Mach number and at a high Reynolds number that is representative of flight conditions. Detailed flowfield measurements of mean and turbulence quantities, in the region from upstream of boundary-layer separation to downstream of wake closure (into the near wake) are made using a laser Doppler velocimeter.

Some of the characteristics of the separated flow may be summarized as follows.

First, fully developed separation, as inferred from γ_p measurements using the low-speed criterion, occurs close to the location at which surface flow reversal is observed; wake closure occurs just downstream of the trailing edge, a feature that may be typical of small-scale separated flows.

Second, in the vicinity of separation and in the separated zone, 1) noticeable streamwise changes in mean and tur-

bulence quantities are observed, although there is considerable reduction in the wall adverse-pressure gradients; 2) the turbulent normal stress term, usually neglected in the boundary-layer approximations, assumes importance away from the wall and is significant to the mean flow development; and 3) the turbulent normal stress contributes appreciably to the turbulence production and, hence, cannot be ignored in the turbulence kinetic-energy-transport equation.

Third, in the separated zone, the nondimensional eddy-viscosity distributions are appreciably less than the Cebeci and Smith values in the outer region, and show only a small variation.

Boundary-layer calculations did not predict separation when used with the measured pressure distributions. Good predictions of separation location are seen with a modified pressure distribution in the vicinity of separation and in the separated region.

The experimental results presented here provide a good data base for guiding turbulence modeling as well as for comparison with predictive methods. A detailed report[15] containing all the measured data and calculated quantities in tabular form is available.

Acknowledgments

The authors are thankful to Drs. R. E. Melnik and H. R. Mead of Grumman Aerospace Corporation for providing us results from the Lag Entrainment Integral Method. Thanks are also due to Mr. M. J. Lanfranco for his assistance in boundary-layer calculations, and to Mr. D. R. Harrison for the design and development of the LDV electronics and computer interfacing hardware.

References

[1] Smith, A.M.O., "Remarks on Fluid Mechanics of the Stall," AGARD-LS-74, 1975.

[2] Chappel, P. D., "Flow Separation and Stall Characteristics of Plane, Constant-Section Wings in Subcritical Flow," *Journal of the Royal Aeronautical Society*, Vol. 72, Jan. 1968, pp. 82-90.

[3] Hurley, F. X., Spaid, F. W., Roos, F. W., Stivers, L. S. Jr., and Bandettini, A., "Detailed Transonic Flow Field Measurements About a Supercritical Airfoil Section," NASA TM X-3244, 1975.

[4] Melnik, R. E., Chow, R., and Mead, H. R., "Theory of Viscous Transonic Flow Over Airfoils at High Reynolds Number," AIAA Paper 77-680, 1977.

[5] Green, J. E., "Some Aspects of Viscous-Inviscid Interactions at Transonic Speeds and Their Dependence on Reynolds Number," AGARD-CP-83-71, 1971.

[6] Lock, R. C., "The Predictions of Viscous Effects on Aerofoils in Transonic Flow," paper for DGLR Symposium, Bad Harzburg, West Germany June 1978.

[7] Lock, R. C., "A Review of Methods for Predicting Viscous Effects on Aerofoils and Wings at Transonic Speeds," AGARD-CP-291, Feb. 1981.

[8] Spaid, F. W. and Hakkinen, R. J., "On the Boundary Layer Displacement Effect Near the Trailing-Edge of an Aft-Loaded Airfoil," *Journal of Applied Mathematics and Physics*, Vol. 28, Fasc. 5, 1977, pp. 941-950.

[9] Melnik, R. E., "Round Table Discussion," AGARD-CP-291, Feb. 1981.

[10] Deiwert, G. S., "Computation of Separated Transonic Turbulent Flows," *AIAA Journal*, Vol. 14, June 1976, pp. 735-740.

[11] Johnson, D. A. and Spaid, F. W., "Measurements of the Boundary Layer and Near Wake of Supercritical Airfoil at Cruise Conditions," AIAA Paper 81-1242, 1981.

[12] Bradshaw, P., Cantwell, B. J., Ferziger, J. H., and Kline, S. J., "Experimental Data Needs for Computational Fluid Dynamics—A Position Paper," 1980-81 AFOSR-HTTM-Stanford Conference on Complex Turbulent Flows: Comparison of Computation and Experiments, Vol. I, Stanford University, Sept. 3-6,1980.

[13] Viswanath, P. R., Cleary, J. W., Seegmiller, H. L., and Horstman, C. C., "Trailing-Edge Flows at High Reynolds Number," AIAA Paper 79-1503, 1979; see also *AIAA Journal*, Vol. 18, Sept. 1980, p. 1059-1065.

[14] Cleary, J. W., Viswanath, P. R., Horstman, C. C., and Seegmiller, H. L., "Asymmetric Trailing-Edge Flows at High Reynolds Number," AIAA Paper 80-1396, 1980.

[15] Viswanath, P. R. and Brown, J. L., "An Experimental Documentation of a Separated Trailing-Edge Flow at a Transonic Mach Number," NASA TM 84290, Nov. 1982.

[16] Viswanath, P. R. and Brown, J. L., "Separated Trailing-Edge Flow at Transonic Mach Number," AIAA Paper 82-0348, 1982.

[17] Cebeci, T., Mosinskis, G. J., and Smith, A.M.O., "Calculation of Separation Points in Incompressible Turbulent Flows," *Journal of Aircraft*, Vol. 9, Sept. 1972, pp. 618-624.

[18] Cook, P. J., McDonald, M. A., and Firmin, M.C.P., "Aerofoil RAE 2822—Pressure Distributions, and Boundary Layer and Wake Measurements," AGARD-AR-138, May 1979.

[19] Simpson, R. L., Strickland, J. H., and Barr, P. W., "Features of a Separating Turbulent Boundary Layer in the Vicinity of Separation," *Journal of Fluid Mechanics*, Vol. 79, March 1977, pp. 553-594.

[20] Simpson, R. L., "Some Important Physical Phenomena in Flows with Separated Turbulent Boundary Layers," *Turbulence in Internal Flows—Turbomachinery and Other Engineering Applications*, edited by S.N.B. Murthy, Hemisphere Publishing Corporation, Washington, D.C., 1977, pp. 311-345.

[21] Meroney, R. N. and Bradshaw, P., "Turbulent Boundary Layer Growth Over a Longitudinally Curved Surface," *AIAA Journal*, Vol. 13, Nov. 1975, pp. 1448-1453.

[22] So, R.M.C. and Mellor, G. L., "An Experimental Investigation of Turbulent Boundary Layers Along Curved Surfaces," NASA CR-1940, 1972.

[23] Delery, J. M., "Investigation of Strong Shock Turbulent Boundary Layer Interaction in 2-D Transonic Flows with Emphasis on Turbulence Phenomena," AIAA Paper 81-1245, 1981.

[24] Cebeci, T. and Smith, A.M.O., *Analysis of Turbulent Boundary Layers*, Academic Press, 1974.

[25] Wilcox, D. C. and Rubesin, M. W., "Progress in Turbulence Modeling for Complex Flow Fields Including Effects of Compressibility," NASA TR-1517, 1980.

[26] Green, J. E., Weeks, D. J., and Broomen, J.W.F., "Prediction of Turbulent Boundary Layers and Wakes in Compressible Flow by a Lag Entrainment Method," RAE Tech. Rept. 72231, 1973.

[27] Spaid, F. W. and Stivers, L. S. Jr., "Supercritical Airfoil Boundary Layer Measurements," AIAA Paper 79-1501, 1979.